Chemical Engineering Journal 433 (2022) 133636

Contents lists available at ScienceDirect

Chemical Engineering Journal

journal homepage: www.elsevier.com/locate/cej

Photoautotrophic organic acid production: Glycolic acid production by microalgal cultivation

Nam Kyu Kang [a,b], Minsik Kim [c,d], Kwangryul Baek [a], Yong Keun Chang [c,d], Donald R. Ort [a,b,e,f,*], Yong-Su Jin [a,b,g,*]

[a] Carl R. Woese Institute for Genomic Biology, University of Illinois at Urbana-Champaign, Urbana, IL, USA
[b] DOE Center for Advanced Bioenergy and Bioproducts Innovation, University of Illinois at Urbana-Champaign, Urbana, IL, USA
[c] Department of Chemical and Biomolecular Engineering, Korea Advanced Institute of Science and Technology (KAIST), 291 Daehak-ro, Yuseong-gu, Daejeon, Republic of Korea
[d] Advanced Biomass R&D Center, 291 Daehak-ro, Yuseong-gu, Daejeon, Republic of Korea
[e] Department of Crop Sciences, University of Illinois at Urbana-Champaign, Urbana, IL, USA
[f] Department of Plant Biology, University of Illinois at Urbana-Champaign, Urbana, IL, USA
[g] Department of Food Science and Human Nutrition, University of Illinois at Urbana-Champaign, Urbana, IL, USA

ARTICLE INFO

Keywords:
Chlamydomonas reinhardtii
Glycolate dehydrogenase
Glycolic acid
Two-stage continuous culture
Flux balance analysis
Techno-economic analysis

ABSTRACT

Although microalgae produce value-added products, such as lipids, pigments, and polysaccharides using light and carbon dioxide, these intracellular products require costly downstream processes such as extraction and purification. Thus, extracellular products are desirable for economic production. While reported before, the secretion of glycolic acid by microalgal photorespiration has not received attention for industrial applications. We developed a two-stage continuous cultivation system to increase glycolic acid production using a glycolate dehydrogenase (*GYD1*) deficient mutant of *Chlamydomonas reinhardtii* which produces high concentrations of glycolic acid. Specifically, 3% CO_2 was supplied in the first-stage culture for the production of biomass and ambient air (0.03% CO_2) was supplied to the second stage for the production of glycolic acid. As a result, overall glycolic acid productivity reached 82.0 mg L^{-1} d^{-1} at a dilution rate of 0.34 d^{-1}. However, as the pH of the second stage decreased to 4.7 due to the increased glycolic acid production, we controlled the pH of the second stage at pH 6.0, resulting in 122.6 mg L^{-1} d^{-1} of glycolic acid productivity. Flux balance analysis revealed that the experimental glycolic acid production rate was 69% of the theoretical glycolic acid production rate. The deviation might be due to the toxicity of glycolic acid. When a techno-economic analysis was conducted based on the experimental results, the minimum glycolic acid production cost was estimated to be \$31 kg^{-1}, indicating a potential for industrial production. These findings suggest that microalgae can be utilized for the cost-effective industrial production of glycolic acid.

1. Introduction

Microalgae have emerged as an alternative to petrochemicals as a light-driven renewable feedstock [1,2]. Microalgae have been mainly used for the production of biofuels owing to their high lipid contents [3]. In addition, as microalgae consume inorganic compounds, such as carbon dioxide and heavy metals, microalgal bioengineering can resolve environmental pollution and energy problems simultaneously [4–7]. Microalgae can also produce various value-added products such as omega-3, carotenoids, and isoprenoids [8–10]. Nonetheless, because most microalgae-derived bioproducts are intracellular products, complex and costly downstream processes, such as cell disruption, extraction and purification, are necessary [11]. The downstream processes need sophisticated operations and often costly, hindering the development of microalgal industries [12]. Although the production of extracellular products, such as organic acids and exopolysaccharides from microalgae, can simplify the downstream processes, the process for extracellular products has been overlooked due to the low productivity [13].

Organic acids are commodity chemicals with numerous applications for food additives and various polymers [14]. Microalgae can produce extracellular organic acids using fermentative metabolism [15]. Under dark fermentation (anaerobic) conditions, polysaccharides and sugars

* Corresponding authors at: Woese Institute for Genomic Biology, University of Illinois at Urbana-Champaign, Urbana, IL, USA.
E-mail addresses: d-ort@illinois.edu (D.R. Ort), ysjin@illinois.edu (Y.-S. Jin).

https://doi.org/10.1016/j.cej.2021.133636
Received 26 August 2021; Received in revised form 5 November 2021; Accepted 11 November 2021
Available online 17 November 2021
1385-8947/

Nomenclature

D	dilution rate (d^{-1})
P_1	glycolic acid concentration in the first stage of the two-stage continuous culture ($g L^{-1}$)
P_2	glycolic acid concentration in the second stage of the two-stage continuous culture ($g L^{-1}$)
P_f	glycolic acid concentration of a feed stream ($g L^{-1}$)
P_s	glycolic acid concentration in the single-stage continuous culture ($g L^{-1}$)
P_T	glycolic acid concentration of the overall process of the two-stage continuous culture ($g L^{-1}$)
t	time (d)
X_1	biomass concentration in the first stage of the two-stage continuous culture ($g L^{-1}$)
X_2	biomass concentration in the second stage of the two-stage continuous culture ($g L^{-1}$)
X_f	biomass concentration of a feed stream ($g L^{-1}$)
X_s	biomass concentration in the culture of single-stage continuous cultivation ($g L^{-1}$)
X_T	biomass concentration of the overall process of the two-stage continuous culture ($g L^{-1}$)
r_1	specific glycolic acid production rate in the first stage (d^{-1})
r_2	specific glycolic acid production rate in the second stage (d^{-1})
r_s	specific glycolic acid production rate in a single-stage continuous cultivation (d^{-1})
r_T	specific glycolic acid production rate of the overall process in a two-stage continuous culture (d^{-1})

Greek letters

μ_1	specific growth rate of *C. reinhardtii* in the first stage (d^{-1})
μ_2	specific growth rate of *C. reinhardtii* in the second stage (d^{-1})
μ_s	specific growth rate of *C. reinhardtii* in a single-stage continuous cultivation (d^{-1})
μ_T	specific growth rate of *C. reinhardtii* in a two-stage continuous culture (d^{-1})

are catabolized to generate chemical energy (ATP) with reductant (NADH and NADPH) [16]. The accumulated reductant can be used by metabolizing pyruvate to several end-products including organic acids (formate, acetate, and lactate) [17]. However, as the anaerobic organic acid production by microalgae is not sustainable but transient, industrial production of organic acids based on the fermentative process is not economically feasible.

On the other hand, microalgae can produce glycolic acid using not the fermentative metabolism but the light-driven photorespiration mechanism [18,19]. RuBisCO mainly fixes CO_2 to make sugars and metabolites, but also fixes O_2, forming one molecule each of 3-phosphoglycerate and glycolate [20]. Thus, microalgae can produce increasingly greater amounts of glycolic acid as the ratio of CO_2 and O_2 decreases [19]. Glycolic acid, which is toxic to cells if accumulated at high concentrations, is converted to 3-phosphoglycerate and CO_2 via a photorespiratory pathway [21]. As the first step of the photorespiratory pathway is to convert glycolate to glyoxylate by glycolate dehydrogenase, disruption of glycolate dehydrogenase (*GYD1*) in *Chlamydomonas reinhardtii* resulted in the increased production of glycolic acid [22]. As glycolic acid is utilized for a monomer of diverse biodegradable polymers, glycolic acid can be widely used in the healthcare, pharmaceutical, cosmetics, and food industries [23]. Thus, glycolic acid production by microalgae is expected to contribute to establishing more sustainable and eco-friendly industries.

Considering industrial production of bioproducts from microalgae, continuous cultivation has many advantages, relative to batch and fed-batch cultivations [24]. As continuous cultivation allows the maintenance of stable cultures with proper cell densities for a long time at steady-state, volumetric biomass productivity in continuous cultivation of microalgae are generally 2.3- to 5-times higher than those in batch cultivation [24,25]. Furthermore, a multi-stage continuous cultivation system makes it possible to enhance the productivity of a bioproduct [26]. As microalgae usually accumulate lipid, carotenoid, and other value-added products under stress conditions [27], a two-stage cultivation method using stress conditions has been used for the induction of value-added products in microalgae [28]. By applying this concept to continuous cultivation, the productivity of a target product can be further improved on top of the increased biomass productivity by the continuous cultivation system [29].

Only a few studies have reported the development of glycolic acid production from microalgae but did not examine the economic feasibility of the overall process [18,30]. In this study, we aimed to develop the economical production of glycolic acid from microalgae. We first developed a two-stage continuous cultivation system and performed a flux balance analysis (FBA) to understand the efficiency of our cultivation process. We also conducted a techno-economic analysis (TEA) to evaluate the economic feasibility of the process developed in this study. This study suggests that photoautotrophic multi-stage continuous cultivation of microalgae can be used for the industrial production of glycolic acid.

2. Material and methods

2.1. Microalgae strains and pre-culture

Chlamydomonas reinhardtii strains CC-4349 (CW15 mt-), CC-2702 (CIA5 deficient mutant) and CC-4160 (GYD1 deficient mutant), and CC-400 (CW15 mt+, parental strain of CC-4160) were purchased from *Chlamydomonas* Resource Center (https://www.chlamycollection.org/). The strains were maintained on Tris-Acetate-Phosphate (TAP) agar medium, which consisted of 20 mM Tris-HCl (pH 7.0), 0.375 g L^{-1} NH_4Cl, 0.1 g L^{-1} $MgSO_4·7H_2O$, 0.05 g L^{-1} $CaCl_2·2H_2O$, 0.0108 g L^{-1} K_2HPO_4, 0.0054 g L^{-1} KH_2PO_4, 1 mL L^{-1} glacial acetic acid and 1 mL L^{-1} Hutner's trace elements (50 g L^{-1} $Na_2EDTA·2H_2O$, 22 g L^{-1} $ZnSO_4·7H_2O$, 11.4 g L^{-1} H_3BO_3, 5.06 g L^{-1} $MnCl_2·4H_2O$, 1.61 g L^{-1} $CoCl_2·6H_2O$, 1.57 g L^{-1} CuSO4··$5H_2O$, 1.10 g L^{-1} $(NH_4)_6Mo_7O_{24}·7H_2O$, and 4.99 g L^{-1} $FeSO_4·7H_2O$), at 25 °C under 120 µmol photons m^{-2} s^{-1} constant light. The strains were activated in TAP broth medium at 25 °C under 120 µmol photons m^{-2} s^{-1} constant light with shaking at 120 rpm and were then used as inoculum for cultivation. CC-4349, CC-2702, and CC-400 were pre-cultured for 5 days, and CC-4160 were pre-cultured for 2 weeks.

2.2. Batch cultivation

In batch cultivation, cells were cultivated in HS medium, which consisted of 0.5 g L^{-1} NH_4Cl, 0.02 g L^{-1} $MgSO_4·7H_2O$, 0.01 g L^{-1} $CaCl_2·2H_2O$, 1.44 g L^{-1} K_2HPO_4, 0.72 g L^{-1} KH_2PO_4, and 1 mL L^{-1} Hutner's trace elements. Cultures were conducted in 250 mL Erlenmeyer flasks with 200 mL working volumes at 25 °C under 120 µmol photons m^{-2} s^{-1} constant light with shaking at 120 rpm. Air with 3% CO_2 was supplied to the culture directly at a constant flow of 0.5 vvm (volume gas per volume medium per minute) for the first 6 days to induce photosynthesis and growth, and subsequently ambient air without additional CO_2 was added to induce photorespiration and glycolic acid production. CC-4349, CC-2702, and CC-4160 were cultured under batch conditions for 20 days.

2.3. Single-stage continuous cultivation system

Single-stage continuous cultivation was conducted in a 1 L culture bottle with 500 mL working volumes. HS medium was supplied continuously, and the same amount of culture volume was removed using peristaltic pumps (Masterflex L/S, Cole–Parmer, IL, USA), sustaining total culture volume. Continuous cultivation was conducted at 25 °C with the agitation of 200 rpm by magnetic stirrer under 120 μmol photons m^{-2} s^{-1} constant light. Ambient air was supplied to the culture directly at a constant flow of 0.5 vvm. The single-stage continuous culture was operated under five different dilution rates (D) ranging from 0.053 to 0.34 d^{-1}. The steady state of the single-stage continuous culture was determined by stably maintaining biomass and glycolic acid concentrations after a period of at least 2 residnece times ($1/D$) at each dilution rate condition.

The scheme of single-stage continuous cultivation is presented in Fig. 1a. Specific growth rate and biomass productivity of single-stage continuous cultivation were calculated by the following mass balance Eq. (1) [31]:

$$\frac{dX_s}{dt} = DX_f + \mu_s X_s - DX_s \quad (1)$$

where X_f is the biomass concentration of feed stream, X_s is the biomass concentration in the culture of single-stage continuous cultivation, D is the dilution rate, and μ_s is the specific growth rate of single-stage continuous cultivation. As the feed stream (HS medium) has no biomass, X_f can be ignored, and dX_s/dt can be zero at a steady state. Accordingly, the Eq. (1) can be simplified to:

$$\frac{dX_s}{dt} = (\mu_s - D)X_s = 0 \quad (2)$$

$$\mu_s = D \quad (3)$$

Thus, the specific growth rate is the same as the dilution rate at a steady state in single-stage continuous cultivation as Eq. (3). Biomass productivity at a steady state is calculated by multiplying biomass concentration (X_s) by specific growth rate (μ_s).

Glycolic acid production rate and glycolic acid productivity of single-stage continuous cultivation were calculated by the following mass balance Eq. (4):

$$\frac{dP_s}{dt} = DP_f + r_s P_s - DP_s \quad (4)$$

where P_f is the glycolic acid concentration of feed stream, P_s is the glycolic acid concertation in the culture of single-stage continuous cultivation, D is the dilution rate, and r_s is the specific glycolic acid

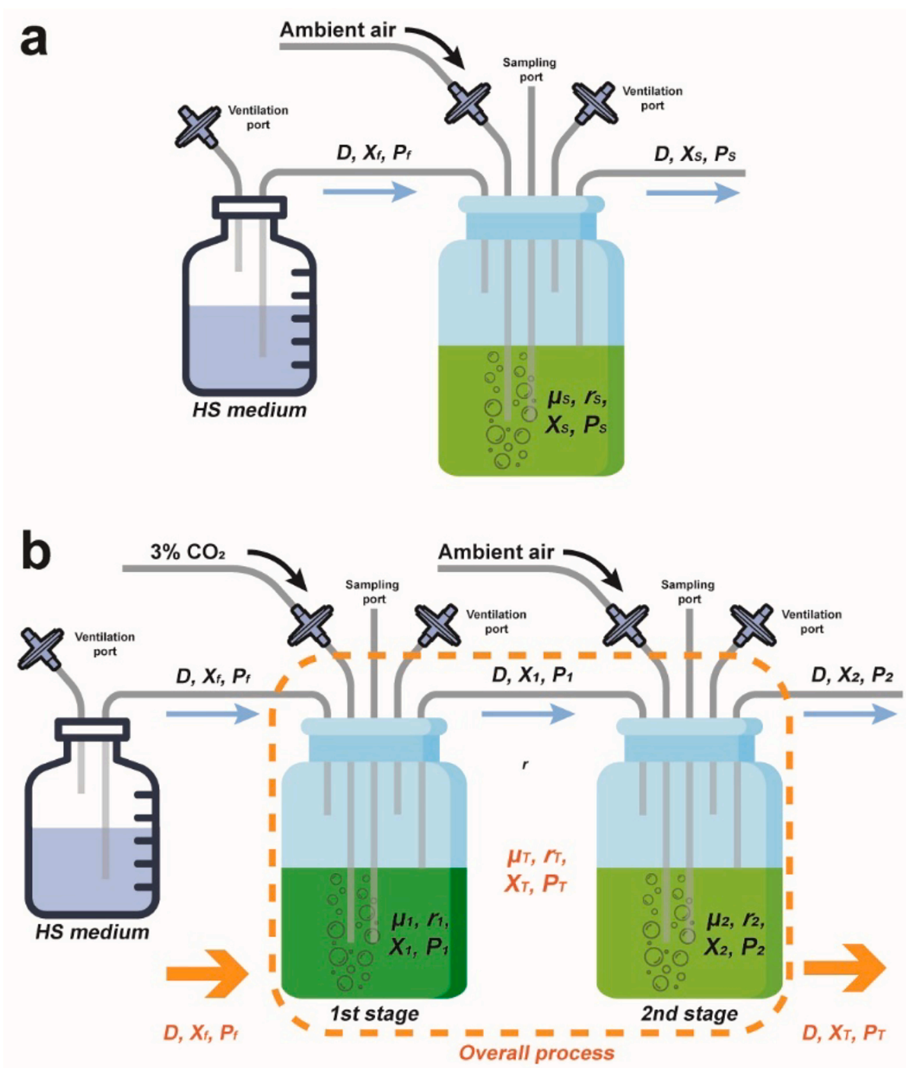

Fig. 1. Scheme of single-stage continuous cultivation (a) and two-stage continuous cultivation (b). In the two-stage continuous cultivation (b), orange-colored arrows, dashed box, and letters represent the process and parameters for calculating biomass and glycolic acid productivity of the overall process.

production rate in single-stage continuous cultivation. As the feed stream (HS medium) has no glycolic acid, P_f can be ignored, and dP_s/dt can be zero at steady state. Accordingly, the Eq. (4) can be simplified to:

$$\frac{dP_s}{dt} = (r_s - D)P_s = 0 \tag{5}$$

$$r_s = D \tag{6}$$

Glycolic acid productivity at a steady state is calculated by multiplying glycolic acid concentration (P_s) in the culture by glycolic acid production rate (r_s) .

2.4. Two-stage continuous cultivation system

In two-stage continuous cultivation, two 1 L culture bottles were connected (Fig. 1b). HS medium was provided to the first stage culture, and the second stage reactor received the culture from the first stage reactor. A working volume of 500 mL in each stage was maintained. Air with 3% CO_2 was supplied to the first stage reactor at 0.5 vvm for biomass production, and ambient air was added to the second stage reactor at 0.5 vvm to induce glycolic acid production. Two-stage continuous cultivation was conducted at 25 °C with agitation 200 rpm by magnetic stirrer under 120 μmol/m^2/s constant light. The two-stage continuous cultures were operated at the dilution rates of 0.17 and 0.34 d^{-1}. The steady states of the two-stage continuous cultures were determined by stably maintaining biomass and glycolic acid concentrations of both stages after a period of at least 4 residence times ($1/D$) at each dilution rate condition. In the case of the pH controlling conditions of the second stage at 0.34 d^{-1}, a steady state was determined after a period of additional 2 residence times.

Specific growth rate and biomass productivity of each stage were calculated separately. The specific growth rate and biomass productivity of the first stage can be calculated by the following mass balance Eq. (7):

$$\frac{dX_1}{dt} = DX_f + \mu_1 X_1 - DX_1 \tag{7}$$

where X_f is the biomass concentration of the feed stream, X_1 is the biomass concentration of the first stage, D is the dilution rate, and μ_1 is the specific growth rate of the first stage. As the feed stream (HS medium) has no biomass, X_f can be ignored, and dX_1/dt can be zero at steady state. Accordingly, the Eq. (7) can be simplified to:

$$\frac{dX_1}{dt} = (\mu_1 - D)X_1 = 0 \tag{8}$$

$$\mu_1 = D \tag{9}$$

Biomass productivity of the first stage at steady state is calculated by multiplying biomass concentration (X_1) by specific growth rate (μ_1) of the first stage.

Glycolic acid production rate and glycolic acid productivity of the first stage was calculated by the following mass balance Eq. (10):

$$\frac{dP_1}{dt} = DP_f + r_1 P_1 - DP_1 \tag{10}$$

where P_f is the glycolic acid concentration of feed stream, P_1 is the glycolic acid concertation of the first stage, D is the dilution rate, and r_1 is the specific glycolic acid production rate of the first stage. As the feed stream (HS medium) has no biomass, P_f can be ignored, and dP_1/dt can be zero at steady state. Accordingly, the Eq. (10) can be simplified to:

$$\frac{dP_1}{dt} = (r_1 - D)P_1 = 0 \tag{11}$$

$$r_1 = D \tag{12}$$

Glycolic acid productivity of the first stage at steady state is calculated by multiplying glycolic acid concentration (P_1) and glycolic acid production rate (r_1) of the first stage.

The specific growth rate and biomass productivity of the second stage can be calculated by the following mass balance Eq. (13):

$$\frac{dX_2}{dt} = DX_1 + \mu_2 X_2 - DX_2 \tag{13}$$

where X_2 and μ_2 are biomass concentration and specific growth rate of the second stage, respectively. As dX_2/dt is zero at steady state, the Eq. (13) can be written as follows:

$$\mu_2 = \frac{D(X_2 - X_1)}{X_2} \tag{14}$$

The biomass productivity of the second stage at steady state is calculated by multiplying biomass concentration (X_2) and specific growth rate (μ_2) of the second stage.

Glycolic acid production rate and glycolic acid productivity of the second stage were calculated by the following mass balance Eq. (15):

$$\frac{dP_2}{dt} = DP_1 + r_2 P_2 - DP_2 \tag{15}$$

where P_2 and r_2 are glycolic acid concentration and specific glycolic acid production rate of the second stage, respectively. As dP_2/dt is zero at steady state, the Eq. (15) can be written as follows:

$$r_2 = \frac{D(P_2 - P_1)}{P_2} \tag{16}$$

Glycolic acid productivity of the second stage at steady state is calculated by multiplying glycolic acid concentration (P_2) by glycolic acid production rate (r_2) of the second stage.

Specific growth rate, biomass productivity, glycolic acid production rate, and glycolic acid productivity of the overall process in two-stage continuous cultivation were calculated assuming that the first and second stages were a single reactor. Specific growth rate and biomass productivity of the overall process were calculated by the following mass balance Eq. (17):

$$\frac{dX_T}{dt} = DX_f + \mu_T X_T - DX_T \tag{17}$$

where μ_T and X_T is the specific growth rate and biomass concentration of the overall process, respectively. As there was no biomass in the feed stream (HS medium), X_f can be ignored and dX_T/dt can be zero at steady state. Accordingly, the Eq. (17) can be simplified to:

$$\frac{dX_T}{dt} = (\mu_T - D)X_T = 0 \tag{18}$$

$$\mu_T = D \tag{19}$$

Biomass productivity of the overall process at steady state was calculated by multiplying biomass concentration (X_T) and specific growth rate (μ_T) of the overall process. As the effluent of the overall process is the same as the effluent of the second stage (Fig. 1b), it can be assumed that the biomass of the overall process (X_T) is equal to the biomass of the second stage (X_2). Thus, the biomass productivity of the overall process was calculated by multiplying biomass concentration (X_2) of the second stage and specific growth rate (μ_T) of the overall process.

Glycolic acid production rate and glycolic acid productivity of two-stage continuous cultivation were calculated by the following mass balance Eq. (20):

$$\frac{dP_T}{dt} = DP_f + r_T P_T - DP_T \tag{20}$$

where r_T and P_T are the specific glycolic acid production rate and glycolic acid concentration of the overall process, respectively. As the feed stream (HS medium) has no glycolic acid, P_f can be ignored, and dP_T/dt

can be zero at steady state. Hence, the Eq. (20) can be simplified to:

$$\frac{dP_T}{dt} = (r_T - D)P_T = 0 \tag{21}$$

$$r_T = D \tag{22}$$

Glycolic acid productivity of the overall process at steady state is calculated by multiplying glycolic acid concentration (P_T) and glycolic acid production rate (r_T) of the overall process. However, for the same reason as calculating the biomass productivity of the overall process, the glycolic acid was calculated by multiplying the glycolic acid concentration of the second stage (P_2) and glycolic acid production rate of the overall process (r_T) .

2.5. Analytical methods

Cell growth was determined by optical density (OD) and biomass concentration. OD was measured at 750 nm using a Biomate 5 ultraviolet–visible spectrophotometer (Thermo Fisher Scientific, Waltham, MA, USA). Biomass concentration was estimated by filtering cells with the MF-Millipore Membrane Filter (0.22 µm pore size, Millipore, MA, USA), washing with deionized water, drying at 75 °C overnight, and measuring the weight of samples. Ammonium concentrations in the medium were measured using the ammonia colorimetric assay kit (K470-100, BioVision, Milpitas, CA, USA), according to the manufacturer's instructions. The concentration of glycolic acid was determined by 1200 Infinity series HPLC system (Agilent Technologies, Santa Clara, CA, USA) equipped with a refractive index detector using a Rezex ROA-Organic Acid H+ (8%) column (Phenomenex Inc., Torrance, CA, USA). The column was eluted with 0.005 N H_2SO_4 at a flow rate of 0.6 mL/min at 50 °C [32].

2.6. Flux balance analyses

In order to conduct *in silico* simulations for estimating upper limits of glycolate production by *C. reinhardtii*, we used the published genome scale metabolic model of *C. reinhardtii*, *i*Cre1355 [33], available at https://github.com/baliga-lab/Chlamy_model_iCre1355. The autotrophic model was used to estimate the theoretical maximum glycolic acid production rate of the *GYD1* mutant. In order to introduce the photorespiration pathway into the *i*Cre1355 model, two transport reactions were added based on Fang et al., (2012) [34]: glycerate transport reactions from mitochondria to cytosol and from cytosol to chloroplast.

To simulate the flux distribution in GYD1 mutant, the reaction of GYD1 was knocked out in the model by setting both upper and lower flux bounds to zero. We set the upper and upper and lower bounds of the RuBisCO carboxylation rate and ammonium uptake rate based on the experimental data of this study (Table S1). The RuBisCO carboxylation rate was estimated using the Eq. (23):

$$CO_2biofixation = \left[\left(C_{biomass} X P_{biomass} \right) + \left(C_{glycolicacid} X P_{glycolicacid} \right) \right] X \left(MCO_2/MC \right) \tag{23}$$

where the symbols stand for $C_{biomass}$-carbon content in the biomass, $P_{biomass}$ -biomass productivity, $C_{glycolic\ acid}$ -carbon content in glycolic acid, $P_{glycolic\ acid}$ -glycolic acid productivity, MCO_2-molar mass of carbon dioxide, and MC -molar mass of carbon [35]. $C_{biomass}$ value was set to 0.52 based on carbon contents of *C. reinhardtii* and other microalgae in previous studies [36,37]. $C_{glycolic\ acid}$ value was set to 0.32 considering the molecular weight of glycolic acid. Experimental values from this study were used for $P_{biomass}$ and $P_{glycolic\ acid}$.

Flux balance analysis (FBA) were performed using Python with the COBRA toolbox. The glpk (GNU Linear Programming kit) package was used to solve linear programming problems [38]. We then estimated the theoretical maximum glycolic acid production rate according to the ratio of the rates of carboxylation and oxygenation (RuBisCO). All code used in the simulation is available in the Supplementary Data 2.

2.7. Techno-economic analysis

The techno-economic analysis was carried out to estimate the glycolic acid production cost of the two-stage continuous cultivation developed in this study. Superpro Designer v9.5 (Intelligen, Inc., Scotch Plains, NJ, USA) was used to calculate the mass and energy balances of the processes.

The following units of the process (Fig. S1) were modeled in Superpro Designer: a blending tank for making medium, a 1-acre open raceway pond (ORP) for pre-culture, two 10-acre ORPs for biomass production and glycolic acid production, a decanter centrifuge, a mixer-settler extractor for glycolic acid extraction, an evaporator for organic solvent recycling, a spray drying, three heat exchangers, four centrifugal pumps, three centrifugal compressors, four mixer/splitters, a gas receiver tank, and three air compressor (Fig. S1).

The total capital cost is calculated as the sum of direct and indirect cost based on values of Superpro designer v9.5. The annualized capital cost is calculated by multiplying the total capital cost by the capital recovery factor (CRF), which can be calculated as follows [39]:

$$\mathrm{CRF} = \frac{i(1+i)^N}{(1+i)^N - 1} \tag{24}$$

where i and N represent the interest rate and the plant lifetime, respectively. In this study, the value of i and N was assumed to be 8% and 20 years, respectively [40]. The material cost and utility cost were estimated based on the simulation results and unit prices of the chemicals and utilities. The labor cost is estimated using the following correlation equation [40]:

$$\text{Labor cost} = 10^6 \times \left(\frac{\text{Total capital cost}}{10^6 \times 500} \right)^{0.2} \tag{25}$$

The maintenance cost was estimated to be 4% of the total capital cost and the laboratory cost for quality control and assurance (Laboratory QC/QA) was estimated to be 8% of the labor cost [41]. The annual operating cost was calculated as the sum of material cost, utility cost, labor cost, maintenance, and Laboratory QC/QA cost. Finally, the annual cost was defined as the sum of the annualized capital cost and the annual operating cost. The glycolic acid production cost was defined as follows [42]:

$$\text{Glycolic acid production cost} = \frac{\text{Annual cost}}{\text{Annual production rate of glycolic acid}} \tag{26}$$

3. Results and discussion

3.1. Screening of glycolic acid producing strains in a batch culture

We cultivated *C. reinhardtii* CIA5 mutant (CC-2702), GYD1 mutant (CC-4160), and CW15 mt- (CC-4349) as a control in a batch culture. For the first 6 days, air with 3% CO_2 was added to induce photosynthesis and biomass production, and then ambient air without additional CO_2 was provided to induce photorespiration and glycolic acid production. We found that CW15 mt- grew well and did not produce extracellular glycolic acid at all (Fig. 2a and b). In contrast, the CIA5 mutant showed significantly reduced growth and produced 0.28 g L^{-1} of glycolic acid in 20 days (Fig. 2a and b). The GYD1 mutant showed slightly reduced growth, relative to WT, and produced 0.72 g L^{-1} of glycolic acid. (Fig. 2a and b). The mutation in *Cia5* which is a master transcriptional regulator of the carbon concentrating mechanism (CCM) negatively affected carbon assimilation and photosynthesis, resulting in notable growth defects under ambient air conditions. On the other hand, as CCM of the GYD1 mutant is intact, its growth did not decrease substantially as compared

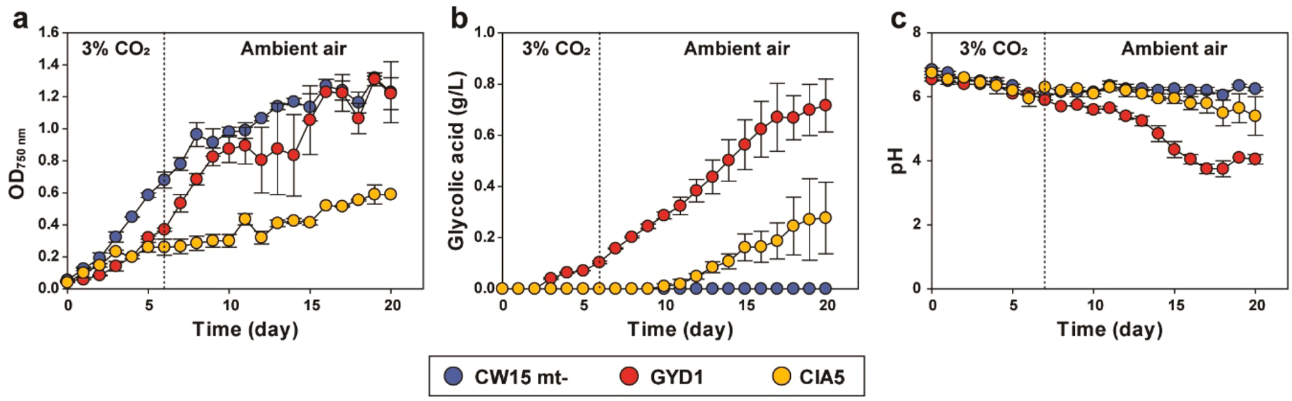

Fig. 2. Analyses of growth, glycolic acid production, and pH in the batch culture. (a) Growth curve based on $OD_{750\ nm}$. (b) Glycolic acid concentration in the culture. (c) pH of the culture. CW15 mt-, GYD1, and CIA5 represents CC-4349 (control), CC-4160 (GYD1 deficient mutant), and CC-2702 (CIA5 deficient mutant), respectively. Cells were cultivated in 250 mL Erlenmeyer flasks with 200 mL working volumes of HS medium at 25 °C, 120 rpm, and 120 μmol photons m^{-2} s^{-1} constant light. Air with 3% CO_2 was provided to the culture for the first 6 days for photosynthesis and growth, and then the ambient air was supplied to the culture for photorespiration and glycolic acid production. The data points represent the average of samples and error bars indicate standard deviation (n = 2).

to the CIA5 mutant. It appeared the slightly reduced growth of the GYD1 mutant was attributed to a pH decrease of the culture medium due to the production of glycolic acid (Fig. 2c).

Taubert et al., (2019) reported the glycolic acid production in *C. reinhardtii* WT via the photorespiration mechanism [18]. They tried to develop the glycolic acid-producing process, combined with a methane production process using anaerobic fermentation of glycolic acid. To produce glycolic acid by *C. reinhardtii*, they used 6-ethoxy-2-benzothiazolesulfonamide (EZA) and isoniazid, which are inhibitors of carbon fixation. Furthermore, they supplied a high concentration of oxygen (40% O_2/0.2% CO_2) to induce photorespiration. Considering an industrial-level production, the use of toxic chemicals and high concentrations of oxygen is not economically feasible. In contrast, the GYD1 mutant can produce a high concentration of glycolic acid under just

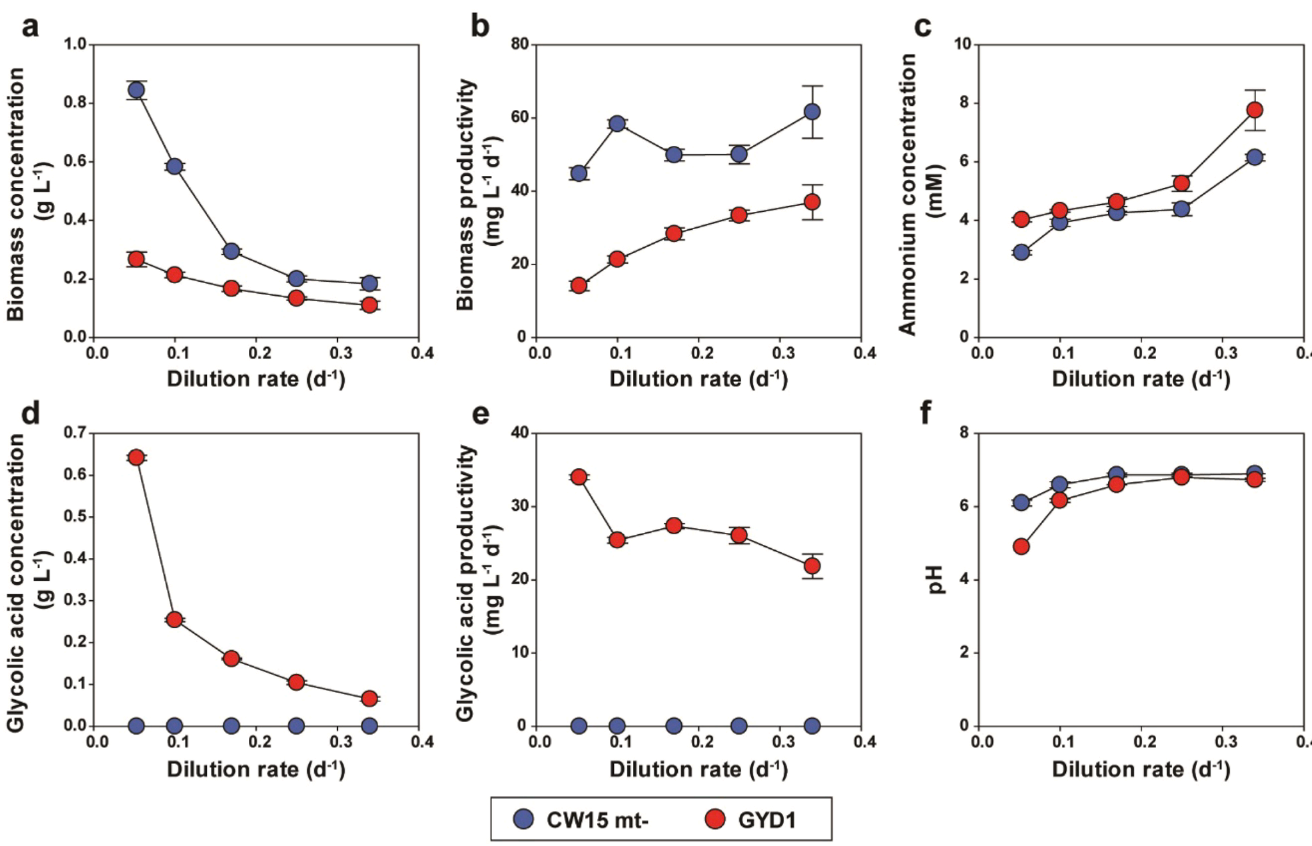

Fig. 3. Analyses of growth, glycolic acid production, pH, and ammonium consumption under single-stage continuous cultivation according to the dilution rate. CW15 mt + and GYD1 represents CC-400 (control) and CC-4160 (GYD1 deficient mutant). (a) Biomass concentration. (b) biomass productivity. (c) ammonium concentration in the culture. (d) glycolic acid concentration. (e) glycolic acid productivity. (f) pH of the culture. Single-stage continuous cultivation was performed in a 1 L culture bottle with 500 mL working volumes. HS medium was provided to the culture according to different dilution rates (0.053, 0.1, 0.17, 0.25, and 0.34 d^{-1}). Single-stage continuous cultivation was conducted at 25 °C with agitation of 200 rpm by magnetic stirrer under 120 μmol photons m^{-2} s^{-1} constant light. Ambient air was directly supplied to the culture at a constant flow of 0.5 vvm. The data points represent the average of samples and error bars indicate standard deviation (n = 3).

ambient air conditions. Accordingly, we decided to delve into cultivation conditions to increase glycolic acid productivity using the GYD1 mutant for industrial production.

3.2. Single-stage continuous cultivation of GYD1 mutant

Single-stage continuous cultivation was conducted with the GYD1 mutant (CC-4160), and CW15 mt+ (WT, CC-400), the parental strain of the GYD1 mutant (Fig. 1a and Fig. S2). Ambient air was provided for the continuous culture to induce photorespiration and glycolic acid production. We confirmed that the performance of glycolic acid production was changed according to dilution rates. The biomass concentrations and biomass productivities of the GYD1 mutant were lower than those of the WT strain at all dilution rates (Fig. 3a and b). This result was consistent with the batch cultivation result. Due to the lower growth, the GYD1 mutant also consumed less ammonium in the HS medium, relative to the WT strain (Fig. 3c). While the biomass concentrations of both WT and GYD1 mutant strains increased as dilution rates decreased (Fig. 3a), biomass productivities of both WT and GYD1 mutant strains decreased (Fig. 3b).

We also found that only the GYD1 mutant secreted glycolic acid (Fig. 3d). The secreted glycolic acid concentration of the GYD1 mutant increased as dilution rates decreased. At the lowest dilution rate (0.053 d^{-1}), the glycolic acid concentration and productivity were 0.64 g L^{-1} and 34.0 mg L^{-1} d^{-1}, which were highest in the single-stage continuous cultivation (Fig. 3d and e). Due to the higher production of glycolic acid at a low dilution rate, the pH of the GYD1 culture decreased to 4.9, while the pH of WT culture was maintained above 6 (Fig. 3f).

However, the highest glycolic acid productivity (34.0 mg L^{-1} d^{-1}) in the single-stage continuous cultivation at the dilution rate of 0.053 d^{-1} (Fig. 3e) was lower than the volumetric productivity (35.8 mg L^{-1} d^{-1}) of glycolic acid in the batch culture (Fig. 2c). When we performed the batch cultivation, we provided 3% CO_2 to the culture in the initial growth stage to increase biomass. Due to the enhanced growth at the early stage, the GYD1 mutant was able to produce more glycolic acid when ambient air was provided. In contrast, as we supplied only ambient air in the single-stage continuous cultivation, the GYD1 mutant did not accumulate biomass to support a large increase of glycolic acid productivity. Thus, the single-stage continuous cultivation has a limitation in enhancing glycolic acid productivity due to slow growth under ambient air conditions.

3.3. Two-stage continuous cultivation of GYD1 mutant

In order to overcome the drawback of low cell densities of the GYD1 mutant in the single-stage continuous cultivation system, two-stage continuous cultivation was implemented (Fig. 1b and Fig. S3). Air with 3% CO_2 was supplied to the first stage for biomass production to induce high rates of net photosynthesis, and ambient air without additional CO_2 was added to the second stage to induce glycolic acid production by the RuBisCO oxygenation reaction.

Under the two-stage continuous culture, the biomass concentration of the first stage was 0.72 g L^{-1} at a dilution rate of 0.17 d^{-1} and 0.50 g L^{-1} at the dilution rate of 0.34 d^{-1} (Fig. 4a). Thus, biomass productivities of the first stage were 121.8 mg L^{-1} d^{-1} and 170.0 mg L^{-1} d^{-1} at the dilution rates of 0.17 d^{-1} and 0.34 d^{-1}. In contrast, the biomass concentrations

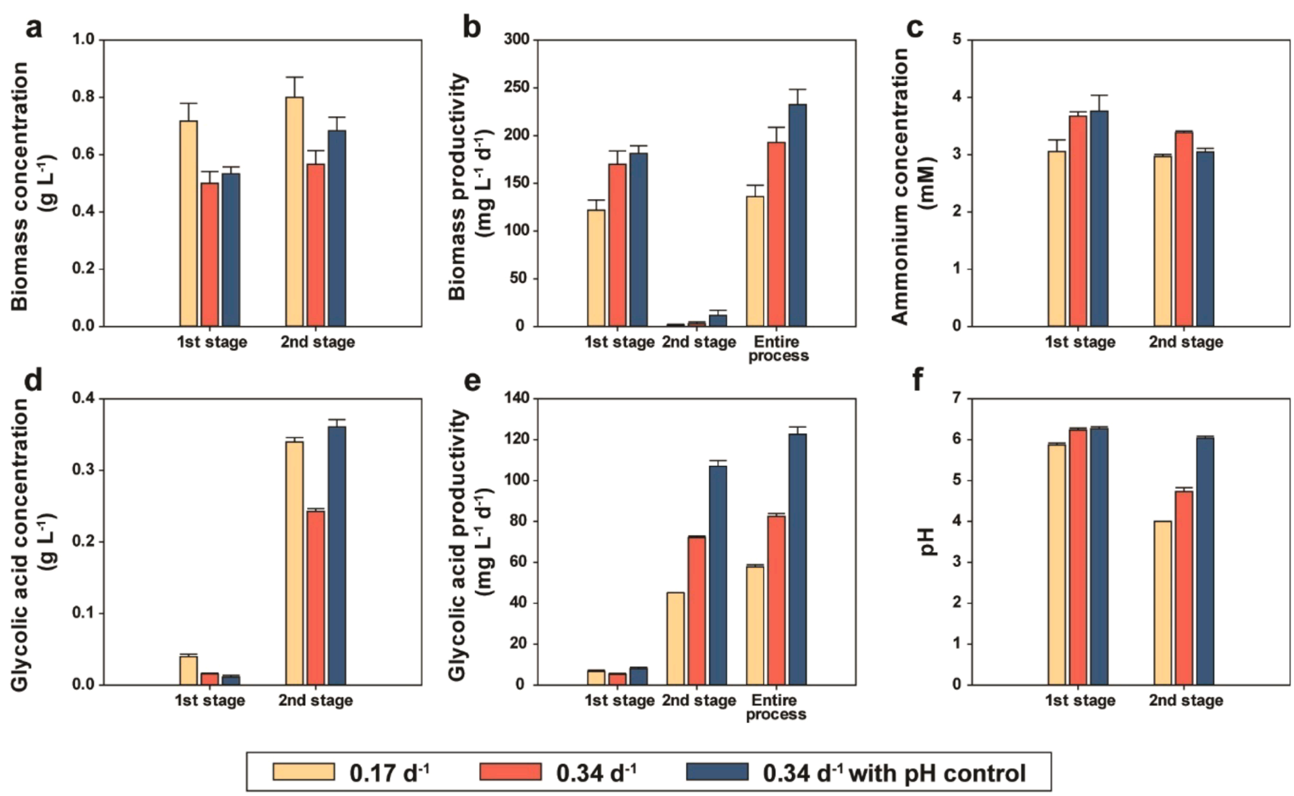

Fig. 4. Analyses of growth, glycolic acid production, pH, and ammonium consumption of GYD1 mutant (CC-4160) in two-stage continuous cultivation. (a) Biomass concentration, (b) biomass productivity, (c) ammonium concentration in the culture, (d) glycolic acid concentration, (e) glycolic acid productivity, and (f) pH of the culture were analyzed at steady state. For two-stage continuous cultivation, two culture bottles were connected. HS medium was provided to the first stage culture using two dilution rates (0.17 d^{-1} and 0.34 d^{-1}), and the second stage reactor received the culture from the first stage reactor. Additionally, growth, glycolic acid production and pH were analyzed with pH control of the second stage at the dilution rate of 0.34 d^{-1}. Working volume of 500 mL in each stage was maintained in continuous culture. Two-stage continuous cultivation was conducted at 25 °C with agitation of 200 rpm by magnetic stirrer under 120 μmol photons m^{-2} s^{-1} constant light. Air with 3% CO_2 and ambient air were directly supplied to the first and second stage culture, respectively, at a constant flow of 0.5 vvm. The data points represent the average of samples and error bars indicate standard deviation (n = 3).

(0.80 g L^{-1} and 0.57 g L^{-1}) in the second stage were only slightly increased over the first stage due to the lack of CO_2, resulting in low biomass productivities of 1.57 mg L^{-1} d^{-1} and 2.92 mg L^{-1} d^{-1} at the dilution rates of 0.17 d^{-1} and 0.34 d^{-1}, respectively (Fig. 4b). The initial ammonium concentration of the HS medium was about 9 mM and a large amount of the supplied ammonium was consumed at the first stage with increased biomass production. We observed that ammonium was barely consumed in the second stage as biomass productivities are 100-fold lower than those at the first stage (Fig. 4c). The biomass productivities of the overall process were 136.0 and 192.7 mg L^{-1} d^{-1} at the dilution rates of 0.17 and 0.34 d^{-1}, respectively. When compared to the single-stage cultivation where only ambient air was used, the overall biomass productivities of the GYD1 mutant were significantly increased, especially at the first stage by using 3% CO_2 (Fig. 3b and 4b).

Glycolic acid production was also improved in the two-stage continuous cultivation system. Although the GYD1 mutant produced only negligible amounts of glycolic acid in the first stage, the GYD1 mutant produced 0.34 and 0.24 g L^{-1} of glycolic acid in the second stage when the dilution rates were 0.17 and 0.34 d^{-1}, respectively (Fig. 4d). Consequently, the glycolic acid productivities of the overall process in two-stage continuous cultivation were 57.8 mg L^{-1} d^{-1} and 82.5 mg L^{-1} d^{-1} at the dilution rates of 0.17 and 0.34 d^{-1}, respectively (Fig. 4e). The productivities in the two-stage continuous cultivation were 70% and 143% higher than those in the single-stage continuous cultivation. The increased biomass productivity in the first stage led to significantly improved glycolic acid production at the second stage.

Besides, we observed that the biomass and glycolic acid productivities were higher at a high dilution rate condition (0.34 d^{-1}). The specific growth rate and glycolic acid production rate of the second stage at the dilution rate of 0.34 d^{-1} were almost doubled, relative to those at the dilution rate of 0.17 d^{-1} (Table 1). The increased growth rate in the second stage might be related to the pH of the culture. The pH of the second stage culture was lower (pH 4.0 vs. 4.7) at the dilution rate of 0.17 d^{-1} than at the dilution rate of 0.34 d^{-1} due to the high concentrations of the glycolic acid in the culture (Fig. 4e and f). The lower pH of the culture negatively affected the cells, resulting in a lower growth rate and glycolic acid production rate (Table 1). Thus, a high dilution rate appeared to be more suitable for the production of glycolic acids.

We also noticed that the pH in the first stage where CO_2 was supplied to suppress photorespiration was maintained at 6 regardless of dilution rates. This indicated that pH 6 is a favorable condition for the GYD1 mutant to grow. Thus, it was expected that glycolic acid production can be further enhanced if the pH of the second stage is maintained at 6.

3.4. Two-stage continuous cultivation of GYD1 mutant with pH control of the second stage

We examined the effects of pH on growth and glycolic acid production by transferring the cells from the continuous culture into batch culture. We collected the outflow GYD1 mutant culture from the second stage of two-stage continuous cultivation with the dilution rate of 0.34 d^{-1}. As the pH of the outflow culture was 4.4, the pHs of the batch culture were adjusted to 4.4 and 6.0, which was the same as the pH of the first stage using 1 N KOH (Fig. 4f). When the GYD1 mutant was cultured at the initial pH 6.0 and 4.4 conditions, the GYD1 mutant maintained the cell density and produced more glycolic acid at the condition of initial pH 6.0 as compared to the conditions with initial pH 4.4 (Fig. S4). This indicated that a decrease in pH due to glycolic acid production negatively affected further growth and glycolic acid production.

Table 1
Specific growth rate and glycolic acid production rate at the second stage of two-stage continuous cultivation.

Rate\Dilution rates	0.17 d^{-1}	0.34 d^{-1}	0.34 d^{-1} with pH control
Specific growth rate (d^{-1})	0.017 ± 0.005	0.040 ± 0.012	0.074 ± 0.016
Specific glycolic acid production rate (d^{-1})	0.150 ± 0.001	0.318 ± 0.001	0.318 ± 0.001

Thus, we controlled the pH of the second stage at the dilution rate of 0.34 d^{-1}. The pH of the second stage was maintained at 6.0 by the automatic addition of 0.5 N KOH (Fig. 4f). As a result, the biomass concentration of the second stage further increased up to 0.68 g L^{-1}, which was 28% higher than that of the first stage (Fig. 4a). Given that biomass concentration of the second stage without pH control exhibited a 13% increase compared to the first stage, biomass production was certainly enhanced by the pH control. Consequently, biomass productivity of the overall process increased to 232.3 mg L^{-1} d^{-1} (Fig. 4b).

The glycolic acid concentration was also enhanced along with the increased biomass production by pH control (Fig. 4d). Thus, glycolic acid productivity of the overall process with pH control was 122.6 mg L^{-1} d^{-1}, which was 49% higher than the productivity under no pH control condition (Fig. 4e). Notably, the glycolic acid productivity was 3.6-fold greater at the dilution rate of 0.34 d^{-1} with pH control compared to the single-stage continuous cultivation (Fig. 3e and 4e).

We also observed that the pH control of the second stage has a positive effect on the specific growth rate rather than glycolic acid production rate (Table 1). As such, the increase of glycolic acid production by pH control might be due to the enhanced growth of the GYD1 mutant.

3.5. Flux balance analysis of the GYD1 mutant

FBA was performed to estimate the theoretical maximum glycolic acid production rate of the GYD1 mutant using the genome scale metabolic model of *Chlamydomonas reinhardtii* iCre1355. The RuBisCO carboxylation rate and the ammonium uptake rate were estimated based on the experimental results of the single-stage continuous cultivation at $D = 0.34$ d^{-1}. The RuBisCO carboxylation rate (CO_2 biofixation rate, eq (23)) was calculated based on only biomass and extracellular glycolic acid [35]. Although the GYD1 mutant could produce other extracellular products from CO_2 [13], the amount seems to be negligible according to the HPLC result (Fig. S5). We set the upper and lower bounds of the RuBisCO carboxylation rate to 0.82 mmol $gDW^{-1}h^{-1}$ and those of the ammonium uptake rate to 0.19 mmol $gDW^{-1}h^{-1}$ (Table S1). The growth rate and glycolic acid production rate were simulated according to the ratio of the rates of carboxylation and oxygenation (CO_2/O_2) reactions by RuBisCO (Fig. 5a). Basically, the growth rate and glycolic acid production rate was inversely proportional. The growth rate increased with increased carboxylation reaction rates, resulting in 0.022 h^{-1}, equal to 0.53 d^{-1}, of the maximum growth rate with the lowest glycolic acid production rate. On the other hand, the glycolic acid production rate increased with increased oxygenation reaction rates, resulting in 0.41 mmol $gDW^{-1}h^{-1}$ of the maximum glycolic acid production rate with the lowest growth rate. At the growth rate of 0.014 h^{-1} (0.35 d^{-1}), the theoretical maximum glycolic acid production rate was calculated to be 0.16 mmol $gDW^{-1}h^{-1}$ (Fig. 5b). The experimental glycolic acid production rate at the dilution rate of 0.014 h^{-1} (0.35 d^{-1}) under the single-stage continuous cultivation was 0.11 mmol $gDW^{-1}h^{-1}$, which showed a 31% deviation between the experimental and predicted values (Fig. 5b). We also investigated theoretical maximum glycolic acid production rates under the two-stage continuous cultivation with or without pH regulation at the dilution rate of 0.35 d^{-1}, and the theoretical maximum glycolic acid production rates were 0.13 and 0.15 mmol $gDW^{-1}h^{-1}$, which had 38% and 33% deviations, respectively (Table S1). The deviations might be caused because FBA does not consider the toxicity of glycolic acid and environmental stresses, such as low pH. Considering the stress factors by glycolic acid, our experimental glycolic acid production rates might be almost the maximum values. We also investigated metabolic fluxes of the photosynthesis and photorespiration pathways in the GYD1 mutant at the growth rate of 0.014 h^{-1} (0.35 d^{-1}), and found

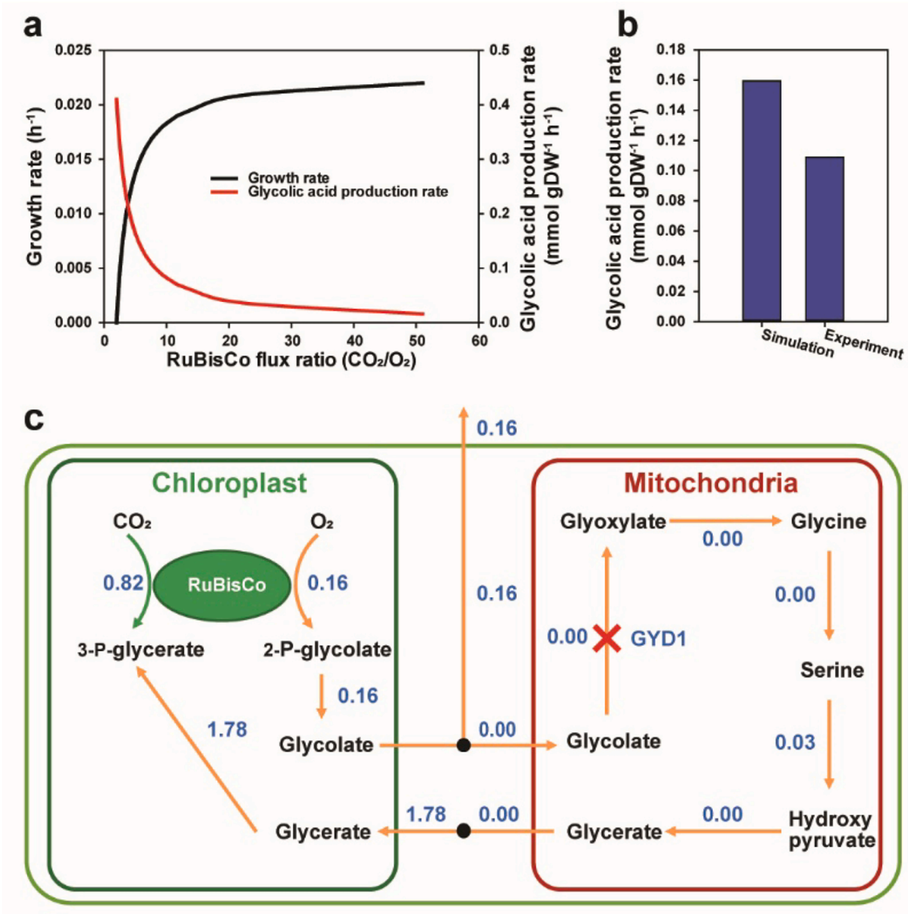

Fig. 5. The flux balance analyses of the GYD1 mutant. (a) Predicted growth rate and glycolic acid production rate of the GYD1 mutant according to rate according to the ratio of the rates of carboxylation and oxygenation (CO_2/O_2) by RuBisCO. The carboxylation flux was fixed with 0.82 mmol $gDW^{-1}h^{-1}$ based on the experimental data, and the oxygenation rate was varied. (b) The simulated and experimental glycolic acid production rate of the GYD1 mutant at the growth rate of 0.014 h^{-1} (0.34 d^{-1}). (c) Predicted metabolic flux distributions of the photosynthesis and photorespiration pathways in the GYD1 mutant via the FBA the growth rate of 0.014 h^{-1} (0.34 d^{-1}). The green arrow and orange arrows represent the photosynthesis and photorespiration pathways, respectively. The unit of flux values is mmol $gDW^{-1}h^{-1}$. (For interpretation of the references to colour in this figure legend, the reader is referred to the web version of this article.)

that all oxygenated fluxes by RuBisCO did not go through the GYD1 reaction, leading to the production of extracellular glycolic acid (Fig. 5c). Based on the FBA result, we confirmed that our continuous processes were well-established for the production of glycolic acid.

3.6. Techno-economic analysis of microalgae-based glycolic acid production

TEA was carried out to evaluate the economic feasibility of glycolic acid production by the GYD1 mutant. We compared three cases of the two-stage continuous cultivation systems (the dilution rates of 0.17 d^{-1}, 0.34 d^{-1}, and 0.34 d^{-1} with pH control) based on the results in this study.

The simulated process consisted of pre-culture, biomass production, glycolic acid production, glycolic acid extraction, glycolic acid drying, and medium and extraction solvent recycling processes (Fig. S1). We modeled the two-stage continuous cultivation system using two open raceway ponds (ORPs). The data of biomass, glycolic acid production, and required major nutrient (NH_4Cl, K_2HPO_4, and KH2PO4) concentration were determined based on the experimental data in this study (Table S2). In the case of other nutrients, initial concentrations of HS medium were used, and trace metal was omitted. In downstream processes, a decanter centrifuge was used to separate cells from supernatants, and a methyl isobutyl ketone (MIBK) solvent and amberlite resin were employed for glycolic acid extraction. We assumed that MIBK solvent was recycled and Amberlite resin was set up with the glycolic acid extraction unit (the mixer-settler extractor), and thereby the Amberlite resin cost was included in the equipment purchase cost. The data of harvesting and extraction of glycolic acid were collected from the available literature [43,44]. The assumption of major parameters applied to the process are presented in Table S3.

The details of the total capital cost and operating cost of the three cases were presented in Table S4 and S5. Total annual cost (the sum of annualized capital cost and operating cost) was \$7.07 million, \$11.71 million, and \$11.75 million under the conditions of 0.17 d^{-1}, 0.34 d^{-1}, and 0.34 d^{-1} with pH control, respectively (Table 2). The annual cost for the production of glycolic acid increased at higher dilution rate conditions. Thus, although the annual production rate of glycolic acid was 16% higher at a high dilution rate of 0.34 d^{-1} compared to a low dilution rate of 0.17 d^{-1}, the glycolic acid production cost was 43% greater at the dilution rate of 0.34 d^{-1} due to the high annual cost. Interestingly, with the addition of pH control at the dilution rate of 0.34 d^{-1}, the annual glycolic acid production was doubled (383 MT yr^{-1}) as compared to the condition of the dilution rate of 0.17 d^{-1} without pH control. Thus, although the annual cost was most expensive at the dilution rate of 0.34 d^{-1} with pH control, the glycolic acid production cost was \$31 kg^{-1} which was the lowest price. Based on these results, it was demonstrated that the two-stage continuous cultivation at a high dilution rate (0.34 d-

Table 2
TEA results for the glycolic acid production in microalgae in two-stage continuous cultivation.

Cost \ Dilution rate	0.17 d^{-1}	0.34 d^{-1}	0.34 d^{-1} with pH Control
Annualized capital cost (\$ yr^{-1})	3,153,386	5,096,243	5,102,028
Annual operating cost (\$ yr^{-1})	3,918,014	6,616,889	6,645,623
Annual cost (\$ yr^{-1})	7,071,400	11,713,132	11,747,651
Annual production rate of glycolic acid (MT yr^{-1})	187	272	383
Glycolic acid production cost (\$ kg^{-1})	38	43	31

^{1}) with pH control is the most economic configuration for glycolic acid production.

However, the efficiencies of glycolic acid production in ORP employed for TEA might be lower than the efficiency from the lab-scale experiments. Thus, we additionally conducted TEA with a scenario of reduced efficiencies (25%, 50%, and 75%) of glycolic acid production at the dilution rate of 0.34 d^{-1} with pH control conditions. Basically, the altered efficiencies did not significantly affect the annual costs (Tables S6 and S7). However, decreases in glycolic acid production efficiency increased the production costs. As a result, the glycolic acid production costs were 41, 60, and 120 $ kg^{-1} at 75%, 50%, and 25% efficiencies, respectively (Fig. 6). Considering that glycolic acid is currently produced by chemical synthesis with no carbon sequestration [45] and the market price is estimated to be around $200 to 350 kg^{-1}, the photoautotrophic production of glycolic acid using microalgae will be economically-feasible with the lower efficiencies.

As there is a growing interest in producing chemicals via microbial fermentation from renewable resources, many metabolic engineering studies for glycolic acid production in bacteria or yeast have been reported. To date, the reported highest glycolic acid titer was 108.2 g L^{-1} and 15.0 g L^{-1} in engineered bacteria (*Escherichia coli*) and yeast (*Kluyveromyces lactis*), respectively [45]. However, bacteria and yeast require sugars and produce other byproducts. Although the glycolic acid titer in this study was 0.36 g L^{-1} in the two-stage continuous cultivation (0.34 d^{-1} with pH control), glycolic acid could be economically produced by using modest CO_2 supplementation in the first stage and ambient air in the second stage (Fig. 4d). Indeed, we found that the CO_2 cost is almost 0% of the total operating cost (Table S5 and S7).

Additionally, the reduced downstream process in glycolic acid production might be an economic advantage. Glycolic acid production from microalgae does not require a cell disruption-related process, unlike other microalgal products. Panis et al., (2016) reported TEA of astaxanthin production process using *Haematococcus pluvialis* [46]. Interestingly, they found that the cell disruption step was highly energy-demanding, accounting for a substantial fraction of the operating cost. Moreover, they concluded that the biological production of astaxanthin could not compete with synthetic astaxanthin due to high production costs.

In this study, we present the photoautotrophic production of glycolic acid by the *C. reinhardtii* GYD1 mutant under the well-controlled environment. However, it is necessary to develop an economic and scalable microalgae culture system, just as the TEA was conducted using open raceway ponds. The GYD1 mutant would not be competitive in the open raceway ponds due to various environmental conditions, stresses, and contamination issues. Thus, we propose that the mutants would be transformed with herbicide resistance genes so that inexpensive and environmentally benign herbicides can be used to suppress competitive contamination [47]. Besides, we assumed many parameters of the downstream processes based on the previous studies (Table S3) due to the lack of experimental data. As these may render the calculated production cost of glycolic acid in the TEA inaccurate or underestimated, experimental developments of the downstream processes will be necessary for the commercial production of glycolic acid from the GYD1 mutant. Nevertheless, we envision that the photoautotrophic production of glycolic acid would be as competitive as other microbial fermentation-based production from sugars as carbon dioxide can be directly converted into glycolic acid [45]. Thus, the developed strategy in this study can be considered for the industrial production of glycolic acid.

4. Conclusions

Here, we developed a microalgal cultivation process for the photoautotrophic production of glycolic acid. We report that the GYD1 mutant of *C. reinhardtii* is a promising candidate for the production of glycolic acid from carbon dioxide. When a single-stage continuous cultivation

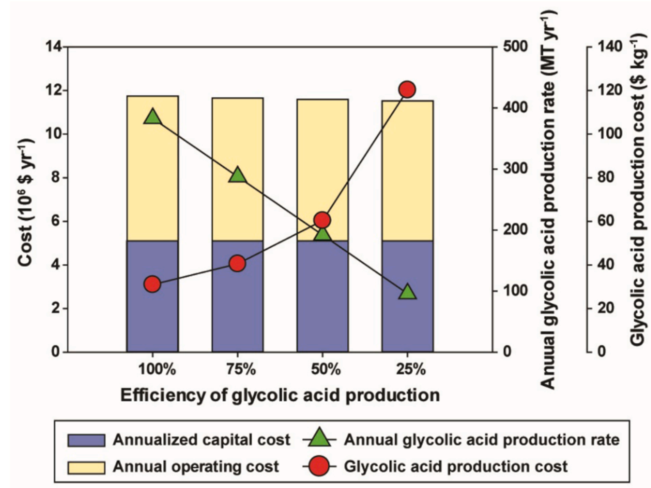

Fig. 6. TEA results according to glycolic acid production efficiency under the 0.34 d^{-1} dilution rate with pH control conditions.

was conducted with the GYD1 mutant by providing ambient air, the GYD1 mutant was not able to sustain the growth and production of glycolic acid. Therefore, we developed a two-stage continuous cultivation of the GYD1 mutant for the efficient production of glycolate. The first stage focused on the growth of the GYD1 mutant by providing 3% CO_2, and subsequently glycolic acid production was induced by providing only ambient air in the second stage. Besides, we controlled the pH of the second stage to further increase glycolic acid production, resulting in a volumetric productivity of 122.62 mg glycolic acid L^{-1} d^{-1}. FBA demonstrated that sustainable production of glycolic acid is feasible and TEA revealed that microalgae-based glycolic acid production can be cost-competitive considering current market prices. These findings suggest that the photoautotrophic production of glycolic acid by a microalgal culture can be conducted at large scales for industrial chemical production and carbon sequestration.

Declaration of Competing Interest

The authors declare that they have no known competing financial interests or personal relationships that could have appeared to influence the work reported in this paper.

Acknowledgments

This work was funded by the Realizing Increased Photosynthetic Efficiency (RIPE) that is funded by the Bill & Melinda Gates Foundation, Foundation for Food and Agriculture Research, and the Department for International Development under grant no. OPP1172157, and the DOE Center for Advanced Bioenergy and Bioproducts Innovation (U.S. Department of Energy, Office of Science, Office of Biological and Environmental Research under award number DE-SC0018420).

Appendix A. Supplementary data

Supplementary data to this article can be found online at https://doi.org/10.1016/j.cej.2021.133636.

References

[1] H.W. Yen, I.C. Hu, C.Y. Chen, S.H. Ho, D.J. Lee, J.S. Chang, Microalgae-based biorefinery–from biofuels to natural products, Bioresour. Technol. 135 (2013) 166–174, https://doi.org/10.1016/j.biortech.2012.10.099.

[2] S. Jeon, B.-R. Jeong, Y.K. Chang, in: Consequences of Microbial Interactions with Hydrocarbons, Oils, and Lipids: Production of Fuels and Chemicals, Springer International Publishing, Cham, 2017, pp. 1–21, https://doi.org/10.1007/978-3-319-31421-1_384-1.

[3] S. Bellou, M.N. Baeshen, A.M. Elazzazy, D. Aggeli, F. Sayegh, G. Aggelis, Microalgal lipids biochemistry and biotechnological perspectives, Biotechnol. Adv. 32 (8) (2014) 1476–1493, https://doi.org/10.1016/j.biotechadv.2014.10.003.
[4] W.S. Chai, W.G. Tan, H.S. Halimatul Munawaroh, V.K. Gupta, S.-H. Ho, P.L. Show, Multifaceted roles of microalgae in the application of wastewater biotreatment: a review, Environ. Pollut. 269 (2021) 116236, https://doi.org/10.1016/j.envpol.2020.116236.
[5] S.Y. Cheng, P.L. Show, B.F. Lau, J.S. Chang, T.C. Ling, New prospects for modified algae in heavy metal adsorption, Trends Biotechnol. 37 (11) (2019) 1255–1268, https://doi.org/10.1016/j.tibtech.2019.04.007.
[6] P.L. Show, S. Thangalazhy-Gopakumar, D.C.Y. Foo, Sustainable technologies for waste reduction and pollutants removals, Clean Technol. Environ. Policy 23 (1) (2021) 1–2.
[7] S.F. Ahmed, M. Mofijur, S. Nuzhat, A.T. Chowdhury, N. Rafa, M.A. Uddin, A. Inayat, T.M.I. Mahlia, H.C. Ong, W.Y. Chia, P.L. Show, Recent developments in physical, biological, chemical, and hybrid treatment techniques for removing emerging contaminants from wastewater, J. Hazard. Mater. 416 (2021) 125912, https://doi.org/10.1016/j.jhazmat.2021.125912.
[8] J. Diao, X. Song, T. Guo, F. Wang, L. Chen, W. Zhang, Cellular engineering strategies toward sustainable omega-3 long chain polyunsaturated fatty acids production: state of the art and perspectives, Biotechnol. Adv. 40 (2020) 107497, https://doi.org/10.1016/j.biotechadv.2019.107497.
[9] L. Novoveská, M.E. Ross, M.S. Stanley, R. Pradelles, V. Wasiolek, J.-F. Sassi, Microalgal carotenoids: a review of production, current markets, regulations, and future direction, Mar. Drugs 17 (11) (2019) 640, https://doi.org/10.3390/md17110640.
[10] J. Wichmann, K.J. Lauersen, O. Kruse, Green algal hydrocarbon metabolism is an exceptional source of sustainable chemicals, Curr. Opin. Biotechnol. 61 (2020) 28–37, https://doi.org/10.1016/j.copbio.2019.09.019.
[11] S. Khanra, M. Mondal, G. Halder, O.N. Tiwari, K. Gayen, T.K. Bhowmick, Downstream processing of microalgae for pigments, protein and carbohydrate in industrial application: a review, Food Bioprod. Process. 110 (2018) 60–84, https://doi.org/10.1016/j.fbp.2018.02.002.
[12] I. Gifuni, A. Pollio, C. Safi, A. Marzocchella, G. Olivieri, Current bottlenecks and challenges of the microalgal biorefinery, Trends Biotechnol. 37 (3) (2019) 242–252, https://doi.org/10.1016/j.tibtech.2018.09.006.
[13] L.u. Liu, G. Pohnert, D. Wei, Extracellular metabolites from industrial microalgae and their biotechnological potential, Mar. Drugs 14 (10) (2016) 191, https://doi.org/10.3390/md14100191.
[14] S.Y. Lee, H.U. Kim, T.U. Chae, J.S. Cho, J.W. Kim, J.H. Shin, D.I. Kim, Y.-S. Ko, W. D. Jang, Y.-S. Jang, A comprehensive metabolic map for production of bio-based chemicals, Nat Catal 2 (1) (2019) 18–33, https://doi.org/10.1038/s41929-018-0212-4.
[15] C. Catalanotti, W. Yang, M.C. Posewitz, A.R. Grossman, Fermentation metabolism and its evolution in algae, Front. Plant Sci. 4 (2013) 150, https://doi.org/10.3389/fpls.2013.00150.
[16] W. Yang, C. Catalanotti, S. D'Adamo, T.M. Wittkopp, C.J. Ingram-Smith, L. Mackinder, T.E. Miller, A.L. Heuberger, G. Peers, K.S. Smith, M.C. Jonikas, A. R. Grossman, M.C. Posewitz, Alternative acetate production pathways in Chlamydomonas reinhardtii during dark anoxia and the dominant role of chloroplasts in fermentative acetate production, Plant Cell 26 (11) (2014) 4499–4518, https://doi.org/10.1105/tpc.114.129965.
[17] C. Catalanotti, A. Dubini, V. Subramanian, W. Yang, L. Magneschi, F. Mus, M. Seibert, M.C. Posewitz, A.R. Grossman, Altered fermentative metabolism in Chlamydomonas reinhardtii mutants lacking pyruvate formate lyase and both pyruvate formate lyase and alcohol dehydrogenase, Plant Cell 24 (2) (2012) 692–707, https://doi.org/10.1105/tpc.111.093146.
[18] A. Taubert, T. Jakob, C. Wilhelm, Glycolate from microalgae: an efficient carbon source for biotechnological applications, Plant Biotechnol. J. 17 (8) (2019) 1538–1546, https://doi.org/10.1111/pbi.2019.17.issue-810.1111/pbi.13078.
[19] A. Gunther, T. Jakob, R. Goss, S. Konig, D. Spindler, N. Rabiger, S. John, S. Heithoff, M. Fresewinkel, C. Posten, C. Wilhelm, Methane production from glycolate excreting algae as a new concept in the production of biofuels, Bioresour. Technol. 121 (2012) 454–457, https://doi.org/10.1016/j.biortech.2012.06.120.
[20] M.E. Dusenge, A.G. Duarte, D.A. Way, Plant carbon metabolism and climate change: elevated CO2 and temperature impacts on photosynthesis, photorespiration and respiration, New Phytol. 221 (1) (2019) 32–49, https://doi.org/10.1111/nph.15283.
[21] P.F. South, A.P. Cavanagh, H.W. Liu, D.R. Ort, Synthetic glycolate metabolism pathways stimulate crop growth and productivity in the field, Sci. 363 (6422) (2019) eaat9077, https://doi.org/10.1126/science.aat9077.
[22] Y. Nakamura, S. Kanakagiri, K. Van, W. He, M.H. Spalding, Disruption of the glycolate dehydrogenase gene in the high-CO2-requiring mutant HCR89 ofChlamydomonas reinhardtii, Can. J. Bot. 83 (7) (2005) 820–833, https://doi.org/10.1139/b05-067.
[23] P.K. Samantaray, A. Little, D.M. Haddleton, T. McNally, B. Tan, Z. Sun, W. Huang, Y. Ji, C. Wan, Poly(glycolic acid) (PGA): a versatile building block expanding high performance and sustainable bioplastic applications, Green Chem. 22 (13) (2020) 4055–4081, https://doi.org/10.1039/D0GC01394C.
[24] B.D. Fernandes, A. Mota, J.A. Teixeira, A.A. Vicente, Continuous cultivation of photosynthetic microorganisms: Approaches, applications and future trends, Biotechnol. Adv. 33 (6 Pt 2) (2015) 1228–1245, https://doi.org/10.1016/j.biotechadv.2015.03.004.
[25] S.H. Ho, X. Ye, T. Hasunuma, J.S. Chang, A. Kondo, Perspectives on engineering strategies for improving biofuel production from microalgae–a critical review, Biotechnol. Adv. 32 (8) (2014) 1448–1459, https://doi.org/10.1016/j.biotechadv.2014.09.002.
[26] H.N. Chang, K. Jung, J.D. Choi, J.C. Lee, H.C. Woo, Multi-stage continuous high cell density culture systems: a review, Biotechnol. Adv. 32 (2) (2014) 514–525, https://doi.org/10.1016/j.biotechadv.2014.01.004.
[27] X.M. Sun, L.J. Ren, Q.Y. Zhao, X.J. Ji, H. Huang, Microalgae for the production of lipid and carotenoids: a review with focus on stress regulation and adaptation, Biotechnol. Biofuels 11 (2018) 272, https://doi.org/10.1186/s13068-018-1275-9.
[28] X.M. Sun, L.J. Ren, Q.Y. Zhao, X.J. Ji, H. Huang, Microalgae for the production of lipid and carotenoids: a review with focus on stress regulation and adaptation, Biotechnol. Biofuels 11 (1) (2018) 272, https://doi.org/10.1186/s13068-018-1275-9.
[29] D.S. Guo, X.J. Ji, L.J. Ren, F.W. Yin, X.M. Sun, H. Huang, G. Zhen, Development of a multi-stage continuous fermentation strategy for docosahexaenoic acid production by Schizochytrium sp, Bioresour. Technol. 269 (2018) 32–39, https://doi.org/10.1016/j.biortech.2018.08.066.
[30] E.J. Yun, G.C. Zhang, C. Atkinson, S. Lane, J.J. Liu, D.R. Ort, Y.S. Jin, Glycolate production by a *Chlamydomonas reinhardtii* mutant lacking carbon-concentrating mechanism, J. Biotechnol. 335 (2021) 39–46, https://doi.org/10.1016/j.jbiotec.2021.06.009.
[31] N.K. Kang, E.K. Kim, M.-G. Sung, Y.U. Kim, B.-R. Jeong, Y.K. Chang, Increased biomass and lipid production by continuous cultivation of Nannochloropsis salina transformant overexpressing a bHLH transcription factor, Biotechnol. Bioeng. 116 (3) (2019) 555–568, https://doi.org/10.1002/bit.v116.310.1002/bit.26894.
[32] T.L. Turner, S. Lane, L.N. Jayakody, G.C. Zhang, H. Kim, W. Cho, Y.S. Jin, Deletion of JEN1 and ADY2 reduces lactic acid yield from an engineered Saccharomyces cerevisiae, in xylose medium, expressing a heterologous lactate dehydrogenase, FEMS Yeast Res. 19 (6) (2019), https://doi.org/10.1093/femsyr/foz050.
[33] S. Imam, S. Schauble, J. Valenzuela, A. Lopez Garcia de Lomana, W. Carter, N.D. Price, N.S. Baliga, A refined genome-scale reconstruction of Chlamydomonas metabolism provides a platform for systems-level analyses, Plant J. 84 (6) (2015) 1239-56, https://doi.org/10.1111/tpj.13059.
[34] W. Fang, Y. Si, S. Douglass, D. Casero, S.S. Merchant, M. Pellegrini, I. Ladunga, P. Liu, M.H. Spalding, Transcriptome-wide changes in Chlamydomonas reinhardtii gene expression regulated by carbon dioxide and the CO2-concentrating mechanism regulator CIA5/CCM1, Plant Cell 24 (5) (2012) 1876–1893, https://doi.org/10.1105/tpc.112.097949.
[35] N. Loira, S. Mendoza, M. Paz Cortés, N. Rojas, D. Travisany, A.D. Genova, N. Gajardo, N. Ehrenfeld, A. Maass, Reconstruction of the microalga Nannochloropsis salina genome-scale metabolic model with applications to lipid production, BMC Systems Biology 11 (1) (2017) 66, https://doi.org/10.1186/s12918-017-0441-1.
[36] C. Hognon, F. Delrue, J. Texier, M. Grateau, S. Thiery, H. Miller, A. Roubaud, Comparison of pyrolysis and hydrothermal liquefaction of Chlamydomonas reinhardtii Growth studies on the recovered hydrothermal aqueous phase, Biomass Bioenergy 73 (2015) 23–31, https://doi.org/10.1016/j.biombioe.2014.11.025.
[37] M. Derakhshandeh, T. Atici, U. Tezcan Un, Evaluation of Wild-Type Microalgae Species Biomass as Carbon Dioxide Sink and Renewable Energy Resource, Waste and Biomass Valorization 12 (1) (2020) 105-121, https://doi.org/10.1007/s12649-020-00969-8.
[38] L. Heirendt, S. Arreckx, T. Pfau, S.N. Mendoza, A. Richelle, A. Heinken, H. S. Haraldsdóttir, J. Wachowiak, S.M. Keating, V. Vlasov, S. Magnusdóttir, C.Y. Ng, G. Preciat, A. Žagare, S.H.J. Chan, M.K. Aurich, C.M. Clancy, J. Modamio, J. T. Sauls, A. Noronha, A. Bordbar, B. Cousins, D.C. El Assal, L.V. Valcarcel, I. Apaolaza, S. Ghaderi, M. Ahookhosh, M. Ben Guebila, A. Kostromins, N. Sompairac, H.M. Le, D. Ma, Y. Sun, L. Wang, J.T. Yurkovich, M.A.P. Oliveira, P. T. Vuong, L.P. El Assal, I. Kuperstein, A. Zinovyev, H.S. Hinton, W.A. Bryant, F. J. Aragón Artacho, F.J. Planes, E. Stalidzans, A. Maass, S. Vempala, M. Hucka, M. A. Saunders, C.D. Maranas, N.E. Lewis, T. Sauter, B.Ø. Palsson, I. Thiele, R.M. T. Fleming, Creation and analysis of biochemical constraint-based models using the COBRA Toolbox v.3.0, Nat. Protoc. 14 (3) (2019) 639–702.
[39] J. Kim, C.A. Henao, T.A. Johnson, D.E. Dedrick, J.E. Miller, E.B. Stechel, C. T. Maravelias, Methanol production from CO2 using solar-thermal energy: process development and techno-economic analysis, Energy Environ. Sci. 4 (9) (2011) 3122–3132, https://doi.org/10.1039/c1ee01311d.
[40] H.Y. Heo, S. Heo, J.H. Lee, Comparative techno-economic analysis of transesterification technologies for microalgal biodiesel production, Ind. Eng. Chem. Res. 58 (40) (2019) 18772–18779, https://doi.org/10.1021/acs.iecr.9b0399410.1021/acs.iecr.9b03994.s001.
[41] T.H. Kwan, D. Pleissner, K.Y. Lau, J. Venus, A. Pommeret, C.S. Lin, Techno-economic analysis of a food waste valorization process via microalgae cultivation and co-production of plasticizer, lactic acid and animal feed from algal biomass and food waste, Bioresour. Technol. 198 (2015) 292–299, https://doi.org/10.1016/j.biortech.2015.09.003.
[42] S. Heo, H.W. Park, J.H. Lee, Y.K. Chang, Design and evaluation of sustainable lactide production process with an one-step gas phase synthesis route, ACS Sustain. Chem. Eng. 7 (6) (2019) 6178–6184, https://doi.org/10.1021/acssuschemeng.8b0638310.1021/acssuschemeng.8b06383.s001.
[43] G. Singh, S.K. Patidar, Microalgae harvesting techniques: a review, J. Environ. Manage. 217 (2018) 499–508, https://doi.org/10.1016/j.jenvman.2018.04.010.
[44] Y.S. Aşçı, I.s. Incı, Extraction of Glycolic Acid from Aqueous Solutions by Amberlite LA-2 in Different Diluent Solvents, J. Chem. Eng. Data 54 (10) (2009) 2791-2794, https://doi.org/10.1021/je800722a.
[45] L. Salusjarvi, S. Havukainen, O. Koivistoinen, M. Toivari, Biotechnological production of glycolic acid and ethylene glycol: current state and perspectives,

Appl. Microbiol. Biotechnol. 103 (6) (2019) 2525–2535, https://doi.org/10.1007/s00253-019-09640-2.

[46] G. Panis, J.R. Carreon, Commercial astaxanthin production derived by green alga Haematococcus pluvialis : A microalgae process model and a techno-economic assessment all through production line, Algal Res. 18 (2016) 175–190, https://doi.org/10.1016/j.algal.2016.06.007.

[47] W.Z. Jiang, D.P. Weeks, A gene-within-a-gene Cas9/sgRNA hybrid construct enables gene editing and gene replacement strategies in Chlamydomonas reinhardtii, Algal Res. 26 (2017) 474–480, https://doi.org/10.1016/j.algal.2017.04.001.